Torsional Optomechanics of a Levitated Nonspherical Nanoparticle

Thai M. Hoang,[1] Yue Ma,[2,3] Jonghoon Ahn,[4] Jaehoon Bang,[4] F. Robicheaux,[1,5]
Zhang-Qi Yin,[2,*] and Tongcang Li[1,4,5,6,†]

[1]*Department of Physics and Astronomy, Purdue University, West Lafayette, Indiana 47907, USA*
[2]*Center for Quantum Information, Institute of Interdisciplinary Information Sciences, Tsinghua University,
Beijing 100084, China*
[3]*Department of Physics, Tsinghua University, Beijing 100084, China*
[4]*School of Electrical and Computer Engineering, Purdue University, West Lafayette, Indiana 47907, USA*
[5]*Purdue Quantum Center, Purdue University, West Lafayette, Indiana 47907, USA*
[6]*Birck Nanotechnology Center, Purdue University, West Lafayette, Indiana 47907, USA*
(Received 12 May 2016; published 15 September 2016)

An optically levitated nanoparticle in vacuum is a paradigm optomechanical system for sensing and studying macroscopic quantum mechanics. While its center-of-mass motion has been investigated intensively, its torsional vibration has only been studied theoretically in limited cases. Here we report the first experimental observation of the torsional vibration of an optically levitated nonspherical nanoparticle in vacuum. We achieve this by utilizing the coupling between the spin angular momentum of photons and the torsional vibration of a nonspherical nanoparticle whose polarizability is a tensor. The torsional vibration frequency can be 1 order of magnitude higher than its center-of-mass motion frequency, which is promising for ground state cooling. We propose a simple yet novel scheme to achieve ground state cooling of its torsional vibration with a linearly polarized Gaussian cavity mode. A levitated nonspherical nanoparticle in vacuum will also be an ultrasensitive nanoscale torsion balance with a torque detection sensitivity on the order of 10^{-29} N m/$\sqrt{\text{Hz}}$ under realistic conditions.

An optically levitated dielectric particle in vacuum [1–3] is an ultrasensitive detector for force sensing [4,5], milli-charge searching [6], and other applications [7,8]. It will provide a great platform to test fundamental theories such as objective collapse models [9,10] and quantum gravity [11] when its mechanical motion can be cooled to the quantum regime [12,13]. Recently, feedback cooling of the center-of-mass (c.m.) motion of a levitated nanosphere to about 450 μK (about 63 phonons at 150 kHz) [14] and cavity cooling of the c.m. motion of a nanosphere to a few mK [15] were demonstrated. The vibration mode would have already been in ground state at 450 μK [14] if its frequency is above 10 MHz. Increasing the vibration frequency of the nanoparticle can be a key to achieve ground state cooling. However, this cannot be achieved by simply increasing the intensity of the trapping laser, which induces heating and subsequently causes the loss of the nanoparticle [4,16]. Besides c.m. motion, a pioneering work has proposed to use multiple Laguerre-Gaussian (LG) cavity modes to achieve angular trapping of a dielectric rod and cool its torsional vibration (TOR) to the ground state [12]. This was later generalized to microwindmills [17], which have better overlap with LG cavity modes. These intriguing proposals of torsional optomechanics, however, have not yet been realized experimentally.

In this work, we report the first experimental observation of the torsional vibration of an optically levitated non-spherical nanoparticle in vacuum, and show that the

torsional frequency can be 1 order of magnitude higher than the c.m. frequency at the same laser intensity. We explain our observation using a model of an ellipsoidal nanoparticle levitated by a linearly polarized Gaussian beam. For an ellipsoid much smaller than the wavelength of the trapping laser, its polarizability is a tensor due to its geometry [18]. In a linearly polarized Gaussian beam, the long axis of an ellipsoid tends to align with the polarization direction of the trapping laser to minimize the potential energy. When its long axis deviates from the polarization direction of the trapping laser, the ellipsoid will experience a torque pushing its long axis back to the equilibrium orientation. As a result, the ellipsoid will experience angular trapping and exhibit torsional vibration. Both the frequency and the quality factor of the torsional vibration can be 1 order of magnitude higher than those of the c.m. motion. Inspired by the experimental observation, we propose a simple yet novel scheme to achieve TOR ground state cooling with a cavity driven by a linearly polarized Gaussian beam. While we use nanodiamonds as examples in this Letter, our proposals will also work for other transparent nonspherical nanoparticles [19,20].

Besides being a platform for investigating fundamental physics, a levitated nonspherical nanoparticle in vacuum will also be a nanoscale torsion balance [21,22]. It can have a torque detection sensitivity on the order of 10^{-29} N m/$\sqrt{\text{Hz}}$ under realistic conditions, which will open up many new applications. Angular trapping and torsional vibration are
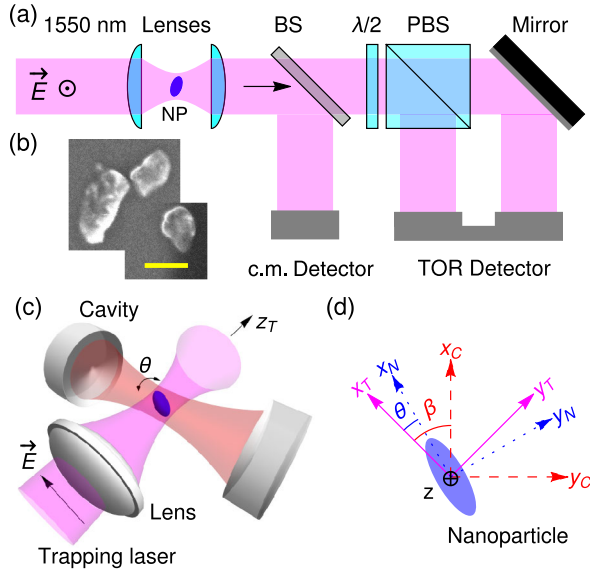
FIG. 1. (a) Experimental diagram for detecting torsional (TOR) vibration and center-of-mass (c.m.) motion of a levitated non-spherical nanoparticle (NP). A nanodiamond (represented by an ellipsoid) is levitated by a tightly focused linearly polarized 1550 nm laser beam. The nanoparticle's motion is monitored by the exiting trapping laser. The exiting beam is split by a beam splitter (BS) to a c.m. detector and a TOR detector. A $\lambda/2$ wave plate balances the power of the beams after the polarizing beam splitter (PBS) for the TOR detector. (b) A SEM image of irregular nanodiamonds. The scale bar is 100 nm. (c) A proposed scheme to cool the torsional vibration of a levitated ellipsoidal nanoparticle with an optical cavity driven by a linearly polarized Gaussian beam. (d) The relation between Cartesian coordinate systems of the nanoparticle (x_N, y_N, z_N), the trapping laser (x_T, y_T, z_T), and the cavity mode (x_C, y_C, z_C). The x_N axis aligns with the longest axis of the nanoparticle. x_T and x_C axes align with the polarization directions of the trapping laser and the cavity mode, respectively. The angle between x_N and x_T is θ, and the angle between x_T and x_C is β. The y_C axis is the optical axis of the cavity. The z_T axis is the propagation direction of the trapping laser. As we consider only one torsional mode, we assume z_C and z_N are parallel to z_T for simplicity.

also important for spin optomechanics of levitated nano-diamonds with nitrogen-vacancy centers [23–27], for which the orientations of nitrogen-vacancy centers are important.

Observation of the torsional vibration of levitated nano-particles.—In the experiment, nanodiamonds are levitated using an optical tweezer formed by a linearly polarized 1550 nm laser beam [Fig. 1(a)]. The laser beam is tightly focused with a N.A. = 0.85 objective lens [27]. The nanodiamonds have broad distributions around their manu-facture size 100 nm. Some nanodiamonds have large aspect ratios, as shown in Fig. 1(b). The torsional vibration of the nanodiamond will change the polarization of the laser beam, which can be detected with a polarizing beam splitter (PBS) and a balanced detector [Fig. 1(a)]. Similar detection schemes have been used to detect the rotation of birefringent particles driven by circularly
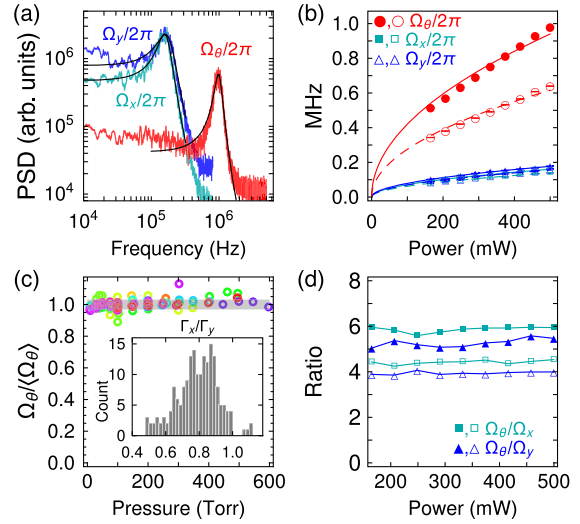

FIG. 2. (a) Measured power spectrum densities (PSD) of the c.m. motion (labeled with $\Omega_{x,y}/2\pi$) and TOR vibration (labeled with $\Omega_\theta/2\pi$) of an optically levitated nanodiamond at 100 Torr. When the power of the trapping laser is about 500 mW, $\Omega_x/2\pi = 0.16\,\text{MHz}$, $\Omega_y/2\pi = 0.18\,\text{MHz}$, and $\Omega_\theta/2\pi = 1.0\,\text{MHz}$. The damping coefficient is anisotropic with a ratio $\Gamma_x/\Gamma_y = 0.69$ for this nanodiamond. (b) Measured TOR and c.m. frequencies of two different nanodiamonds at 100 Torr as a function of the trapping power. Frequency data are fitted to a function $A\sqrt{P}$ with P being the trapping power and A being a fitting parameter. Solid and open symbols represent different nanodiamonds. (c) $\Omega_\theta/\langle\Omega_\theta\rangle$ of 13 nanodiamonds at different pressures. $\langle\Omega_\theta\rangle$ is the average over different pressures of a nanodiamond's torsional frequency. The shaded region is the standard deviation of all $\Omega_\theta/\langle\Omega_\theta\rangle$ data. The inset plot is the histogram of the measured ratios of damping coefficients in x and y directions (Γ_x/Γ_y) for these nanodiamonds at many different trapping powers and pressures. $\Gamma_x/\Gamma_y < 1$ indicates that the long axes of the nanodiamonds align with the polarization direction (x axis) of the laser beam. (d) The ratio $\Omega_\theta/\Omega_{x,y}$ of two levitated nanodiamonds [shown in (b)] at different laser powers.

polarized lasers [28–30]. The c.m. motion of the nano-diamond changes the direction of the laser beam and can be detected with a balanced detector [31,32].

A sample of the power spectrum density (PSD) of the c.m. motion and the TOR motion of a levitated nano-diamond is shown in Fig. 2(a). Over 1/3 of our trapped nanodiamonds exhibit torsional signals. For this nano-diamond, the TOR frequency ($\Omega_\theta/2\pi = 1.0$ MHz) is about 6 times higher than the transverse c.m. frequency ($\Omega_x/2\pi = 0.16$ MHz and $\Omega_y/2\pi = 0.18$ MHz), which is promising for ground state cooling. For comparison, a factor of 6 increase in the c.m. frequency would require the laser power to be increased by a factor of 36, which can induce significant heating of the nanoparticle.

We investigated the motions of many different nanodia-monds as a function of trapping powers [Figs. 2(b) and 2(d)] and air pressures [Fig. 2(c)]. For each nanodiamond exhibiting torsional vibration, the TOR frequency is proportional to the

square root of the trapping power, $\Omega_\theta \propto \sqrt{P}$, as shown in Fig. 2(b). This observation agrees with the prediction of the ellipsoidal model discussed below. Since the c.m. frequency is also proportional to the square root of the trapping power, $\Omega_y \propto \sqrt{P}$, the ratio $\Omega_\theta/\Omega_{x,y}$ is independent of the trapping power, as shown in Fig. 2(d). The TOR frequency is independent of the air pressure, as shown in Fig. 2(c), when the pressure is reduced from atmospheric pressure to a few Torr. The summary of 13 nanodiamonds yields $\Omega_\theta/\langle\Omega_\theta\rangle = 1 \pm 0.03$ across the whole pressure range. Here $\langle\Omega_\theta\rangle$ is the averaged torsional frequency over different pressures for each particle. For comparison, the rotational frequency of a birefringent microsphere driven by a circularly polarized laser is linearly proportional to the laser power, and increases when the air pressure decreases [30], which is very different from our results of the torsional vibration.

Further experimental evidence that supports the interpretation of torsional vibration instead of free rotation is from the measured damping factors which are anisotropic. The measured ratios Γ_x/Γ_y for all the nanoparticles in Fig. 2(c) at different pressures and trapping powers yield a mean value of 0.8. A nonspherical nanoparticle rotating in the xy plane should yield $\Gamma_x/\Gamma_y = 1$ on average [33]. $\Gamma_x/\Gamma_y < 1$ means the long axes of the nanoparticles align with the polarization direction (x axis) of the trapping laser [34].

Ellipsoidal model.—As a minimal model to describe the torsional vibration of an irregular nanodiamond [Fig. 1(b)], we consider an ellipsoid with semiaxes $r_x > r_y = r_z$ in a linearly polarized optical tweezer. When the size of the ellipsoid is much smaller than the wavelength of the laser, we can use the Rayleigh approximation. The induced dipole will be $\mathbf{p} = \alpha_x E_x \hat{\mathbf{x}}_N + \alpha_y E_y \hat{\mathbf{y}}_N + \alpha_z E_z \hat{\mathbf{z}}_N$, where the instantaneous electric field of the laser beam $\mathbf{E}$ is decomposed into components along the principle axes of the ellipsoid [18]. Here, α_x, α_y, α_z are polarizabilities along the principle axes. The force and torque on the ellipsoid are $\mathbf{F} = \langle\nabla(\mathbf{p}\cdot\mathbf{E})\rangle/2$ and $\mathbf{M} = \langle\mathbf{p}\times\mathbf{E}\rangle$, respectively [18,35]. To capture the essential properties of the system, we consider only the c.m. motion of the ellipsoid along the y_T axis and the torsional vibration of the ellipsoid around the z_T axis [Fig. 1(d)]. The potential energy of the ellipsoid in the optical tweezer is

$$U(y,\theta) = -\frac{V}{2c}[\chi_x - (\chi_x - \chi_y)\sin^2\theta]I_L(y), \quad (1)$$

where $V = 4\pi r_x r_y r_z/3$ is the volume of the ellipsoid, c is the speed of light, $\chi_x = \alpha_x/(\epsilon_0 V)$ and $\chi_y = \alpha_y/(\epsilon_0 V)$ are the effective susceptibility of the ellipsoid, ϵ_0 is the vacuum permittivity, θ is the angle between the longest axis of the ellipsoid and the electric field of the laser beam, and $I_L(y)$ is the laser intensity at the location of the ellipsoid. As an example, $\chi_x = 2.05$, $\chi_y = 1.74$ for an ellipsoidal nanodiamond with $r_y/r_x = 0.8$.
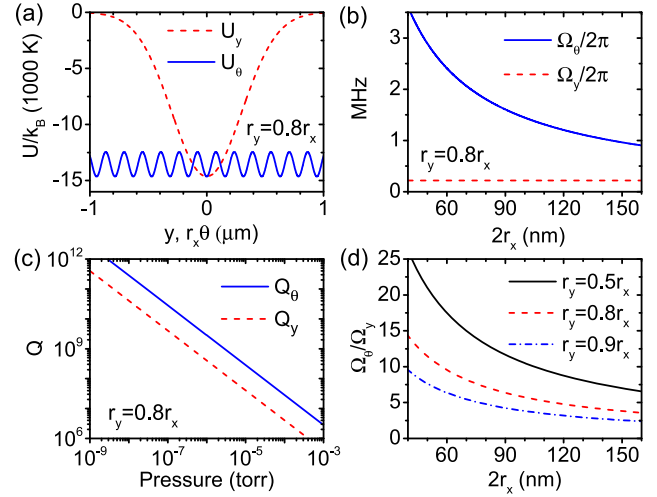

FIG. 3. (a) Trapping potentials in the transverse (U_y) and angular (U_θ) directions. (b) Frequencies of the TOR and c.m. vibrations as a function of the size of the ellipsoid when its aspect ratio is $r_y/r_x = 0.8$. (c) Quality factors of the TOR vibration and c.m. motion of a levitated nanoparticle as a function of the pressure. (d) Enhancement ratio Ω_θ/Ω_y as a function of the size of the ellipsoid with different aspect ratios. In the calculations, we assume the waist of the Gaussian optical tweezer to be 600 nm, the laser wavelength to be 1550 nm, and the laser power to be 100 mW. To calculate results shown in (a) and (c), we assume the semiaxes of the ellipsoid to be $r_x = 50$ nm and $r_y = r_z = 40$ nm. The corresponding vibration frequencies are $\Omega_\theta/2\pi = 1.26$ MHz and $\Omega_y/2\pi = 220$ kHz.

The trapping potential U_y as a function of the transverse position y of an ellipsoid with orientation $\theta = 0$ and the potential U_θ as a function of $r_x\theta$ when $y = 0$ are shown in Fig. 3(a). The semiaxes of the diamond ellipsoid are $r_x = 50$ nm and $r_y = r_z = 40$ nm. To plot U_θ and U_y together, we use $r_x\theta$, the distance the apex point moves, as the horizontal axis for U_θ. While the c.m. potential energy U_y has a Gaussian shape reflecting the spatial profile of the Gaussian laser beam, the torsional potential energy U_θ is a sinusoidal function of the angle θ, as illustrated in Eq. (1). U_θ has several periods within the range of $|r_x\theta| < W_t$. Here, W_t is the waist of the trapping laser. Thus, we expect the torsional vibration to have a higher frequency than that of the c.m. motion. The frequencies of the TOR vibration and c.m. motion of the ellipsoid calculated from the potential energy [Eq. (1)] are

$$\Omega_y = \sqrt{\frac{4\chi_x P}{c\pi\rho W_t^4}}, \qquad \Omega_\theta = \sqrt{\frac{10(\chi_x - \chi_y)P}{c\pi\rho W_t^2(r_x^2 + r_y^2)}}. \quad (2)$$

Here ρ is the particle mass density and P is the power of the Gaussian trapping laser. The ratio Ω_θ/Ω_y scales as W_t/r_x with the semiaxis of the nanoparticle r_x typically 10–20 times smaller than the laser waist W_t.

While the frequency of the c.m. motion is independent of the size of the ellipsoid, the frequency of the torsional vibration increases when the size of the ellipsoid decreases [Fig. 3(b)]. Both experimental (Fig. 2) and theoretical results [Figs. 3(b) and 3(d)] demonstrate that the TOR frequency can be 1 order of magnitude higher than the c.m. frequency at the same laser intensity. The ratio Ω_θ/Ω_y can be increased by decreasing the ratio r_y/r_x or the particle size. Because of a higher frequency, the quality factor of the TOR vibration (Q_θ) [36] can also be 1 order of magnitude higher than that of the c.m. motion (Q_y) [34], which is another advantage for torsional ground state cooling [Fig. 3(c)]. In the calculation, we assume the collisions between air molecules and the ellipsoidal nanoparticle are mainly inelastic, with a momentum accommodation coefficient of 0.9 [34,36].

Torque sensing.—An optically levitated ellipsoid in vacuum will be an ultrasenstive nanoscale torsion balance [37] using the laser as a "string" to provide the restoring torque. Torsion balances have played historic roles in the development of modern physics. They were used in Coulomb's experiment that discovered the law of electrostatic force, the Cavendish experiment that measured the gravitational constant [37], and many other important experiments [38–40]. The minimum torque that can be detected with a torsion balance is $M_{\min} = \sqrt{4k_BTI\Omega_\theta/(Q_\theta\Delta t)}$ [41]. Here T is the environmental temperature, I is the moment of inertia, and Δt is the measurement time. For a levitated $r_x = 50$ nm, $r_y = r_z = 40$ nm ellipsoid at 10^{-8} Torr with a torsional frequency of $\Omega_\theta/2\pi = 1.26$ MHz, the torque sensitivity is about 2×10^{-29} Nm/$\sqrt{\text{Hz}}$ at 300 K. This is several orders more sensitive than tethered nanoscale torque sensors, which typically have sensitivities on the order of 10^{-21} Nm/$\sqrt{\text{Hz}}$ [21,22]. This system can be used to measure the torque on a single electron spin [42] or even a single nuclear spin. A proton in a 0.1 T magnetic field would experience a torque on the order of 10^{-27} Nm.

Torsional ground state cooling.—Inspired by the experimental observation and the ellipsoidal model, we propose to use a linearly polarized Gaussian beam to drive a cavity to cool the torsional vibration to the ground state [12,13,43]. We assume the nonspherical nanoparticle is levitated using another linearly polarized Gaussian beam [Figs. 1(c) and 1(d)]. Because the TOR vibration and c.m. motion can have very different frequencies, we can neglect their coupling. For simplicity, we consider only the torsional mode Ω_θ around the z_T axis. The linear Hamiltonian of the system in the frame rotating at the cooling laser frequency can be approximated as [12,43]

$$\hat{H} = -\hbar\Delta_L\hat{a}^\dagger\hat{a} + \hbar\Omega_\theta\hat{b}^\dagger\hat{b} + \hbar|\alpha|g_\theta(\hat{b}^\dagger + \hat{b})(\hat{a}^\dagger + \hat{a}). \quad (3)$$

Here $2\pi\hbar$ is the Planck constant, $\Delta_L = \omega_L - \omega_C + 2g_\theta^2|\alpha|^2/\Omega_\theta$ is the effective detuning, ω_L is the laser frequency, ω_C is the
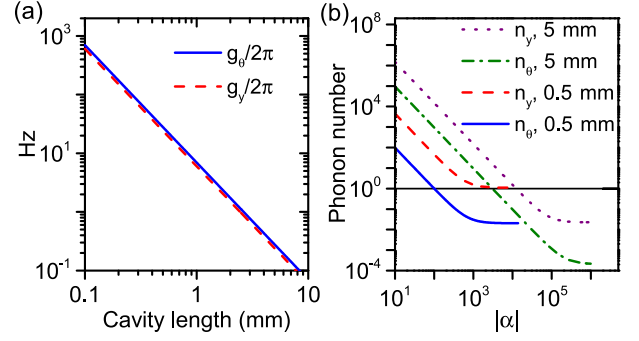

FIG. 4. (a) The single phonon–single photon coupling strengths of the c.m. motion (g_y) and torsional vibration g_θ as a function of cavity length. For the calculation, we assume the size of the diamond ellipsoid to be $r_x = 50$ nm and $r_y = r_z = 25$ nm. The trapping laser parameters are the same as in Fig. 3. The calculated vibration frequencies are $\Omega_\theta/2\pi = 2.6$ MHz and $\Omega_y/2\pi = 248$ kHz. (b) The final phonon numbers of the c.m. mode (n_y) and the torsional mode (n_θ) as a function of the driving field. The resonant wavelength of the cavity is 1540 nm, which is different from that of the trapping laser. The background pressure is assumed to be 10^{-8} Torr. The cavity finesse is $\mathcal{F} = 10^5$.

cavity resonant frequency, $\hat{a}^\dagger$ ($\hat{a}$) and $\hat{b}^\dagger$ ($\hat{b}$) are the creation (annihilation) operators for the cavity field and the mechanical motion, respectively, $|\alpha| = \sqrt{n_p}$ is the steady amplitude of the cavity mode, n_p is the number of photons in the cavity, and g_θ is the coupling strength between a single torsional vibration phonon and a single cavity photon [43]. The coupling strength g_θ will be maximized when the center of the nanoparticle is at the antinode of the cavity mode and the angle between the polarization directions of the trapping laser and the cavity beam is $\beta = 45°$ [Fig. 1(d)]. We obtain the maximum coupling constant as [12,43]

$$g_\theta = \sqrt{\frac{10\hbar\pi r_x r_y^2}{3\rho(r_x^2 + r_y^2)\Omega_\theta}}(\chi_x - \chi_y)\frac{64\pi c}{\lambda_C^2 L^2}. \quad (4)$$

Here λ_C is the wavelength of cavity mode and L is the length of the cavity. The waist of the cavity mode is $W_C = \sqrt{\lambda_C L/2\pi}$ for a confocal cavity.

The single phonon–single photon coupling strength g_θ as a function of the cavity length is shown in Fig. 4(a). For comparison, we also plot the maximum coupling strength between the c.m. motion and the cavity mode, $g_y = \sqrt{2\hbar\pi r_x r_y^2/3\rho\Omega_y}\chi_x(16\pi^2 c/\lambda_C^3 L^2)$, which happens when $\beta = 0°$. For a $r_x = 50$ nm and $r_y = r_z = 25$ nm nanodiamond, g_θ and g_y have similar magnitudes and both increase when the length of the cavity decreases. Using a similar procedure as in Refs. [43,44], we can calculate the steady state phonon number of the levitated nanoparticle. We assume the finesse of the cavity is $\mathcal{F} = 10^5$ and the detuning is $\Delta_L = -\sqrt{(\kappa^2/4) + \Omega_\theta^2}$, with κ being the decay

rate of the cavity. As shown in Fig. 4(b), only the torsional mode can be cooled to the ground state with a $L = 0.5$ mm cavity. For a $L = 5$ mm cavity, both the torsional mode and the c.m. mode can be cooled to the ground states. The torsional vibration mode will have smaller final phonon numbers because of its higher vibration frequency. Thus, the torsional mode can be cooled to the ground state with a broader range of cavity length and driving field strength than those of the c.m. mode. Comparing to former proposals with high-order LG cavity modes [12,17,45], our proposal requires only linearly polarized Gaussian beams. The observed motion is similar to the torsional vibrations ("pendular states") of molecules [46,47] and spins [48] in an external field, and can be used to study torsional decoherence [49].

---

[*]yinzhangqi@mail.tsinghua.edu.cn
[†]tcli@purdue.edu

[1] A. Ashkin and J. M. Dziedzic, Appl. Phys. Lett. **28**, 333 (1976).

[2] T. Li, S. Kheifets, and M. G. Raizen, Nat. Phys. **7**, 527 (2011).

[3] Z.-Q. Yin, A. A. Geraci, and T. Li, Int. J. Mod. Phys. B **27**, 1330018 (2013).

[4] G. Ranjit, D. P. Atherton, J. H. Stutz, M. Cunningham, and A. A. Geraci, Phys. Rev. A **91**, 051805 (2015).

[5] G. Ranjit, M. Cunningham, K. Casey, and A. A. Geraci, Phys. Rev. A **93**, 053801 (2016).

[6] D. C. Moore, A. D. Rider, and G. Gratta, Phys. Rev. Lett. **113**, 251801 (2014).

[7] A. Arvanitaki and A. A. Geraci, Phys. Rev. Lett. **110**, 071105 (2013).

[8] A. D. Rider, D. C. Moore, C. P. Blakemore, M. Louis, M. Lu, and G. Gratta, Phys. Rev. Lett. **117**, 101101 (2016).

[9] O. Romero-Isart, A. C. Pflanzer, F. Blaser, R. Kaltenbaek, N. Kiesel, M. Aspelmeyer, and J. I. Cirac, Phys. Rev. Lett. **107**, 020405 (2011).

[10] O. Romero-Isart, Phys. Rev. A **84**, 052121 (2011).

[11] A. Albrecht, A. Retzker, and M. B. Plenio, Phys. Rev. A **90**, 033834 (2014).

[12] O. Romero-Isart, M. L. Juan, R. Quidant, and J. I. Cirac, New J. Phys. **12**, 033015 (2010).

[13] D. E. Chang, C. A. Regal, S. B. Papp, D. J. Wilson, J. Ye, O. Painter, H. J. Kimble, and P. Zoller, Proc. Natl. Acad. Sci. U.S.A. **107**, 1005 (2010).

[14] V. Jain, J. Gieseler, C. Moritz, C. Dellago, R. Quidant, and L. Novotny, Phys. Rev. Lett. **116**, 243601 (2016).

[15] P. Z. G. Fonseca, E. B. Aranas, J. Millen, T. S. Monteiro, and P. F. Barker, arXiv:1511.08482.

[16] J. Millen, T. Deesuwan, P. Barker, and J. Anders, Nat. Nanotechnol. **9**, 425 (2014).

[17] H. Shi and M. Bhattacharya, J. Mod. Opt. **60**, 382 (2013).

[18] C. F. Bohren and D. R. Huffman, Absorption and Scattering of Light by Small Particles (Wiley-VCH Verlag GmbH, Weinheim, 2007) pp. 130–157.

[19] S. Kuhn, P. Asenbaum, A. Kosloff, M. Sclafani, B. A. Stickler, S. Nimmrichter, K. Hornberger, O. Cheshnovsky, F. Patolsky, and M. Arndt, Nano Lett. **15**, 5604 (2015).

[20] W. Lechner, S. J. M. Habraken, N. Kiesel, M. Aspelmeyer, and P. Zoller, Phys. Rev. Lett. **110**, 143604 (2013).

[21] P. H. Kim, C. Doolin, B. D. Hauer, A. J. MacDonald, M. R. Freeman, P. E. Barclay, and J. P. Davis, Appl. Phys. Lett. **102**, 053102 (2013).

[22] M. Wu, A. C. Hryciw, C. Healey, D. P. Lake, H. Jayakumar, M. R. Freeman, J. P. Davis, and P. E. Barclay, Phys. Rev. X **4**, 021052 (2014).

[23] Z.-Q. Yin, T. Li, X. Zhang, and L. M. Duan, Phys. Rev. A **88**, 033614 (2013).

[24] M. Scala, M. S. Kim, G. W. Morley, P. F. Barker, and S. Bose, Phys. Rev. Lett. **111**, 180403 (2013).

[25] Z.-Q. Yin, N. Zhao, and T. Li, Sci. China Phys. Mech. Astron. **58**, 1 (2015).

[26] L. P. Neukirch, E. von Haartman, J. M. Rosenholm, and A. N. Vamivakas, Nat. Photonics **9**, 653 (2015).

[27] T. M. Hoang, J. Ahn, J. Bang, and T. Li, Nat. Commun. **7**, 12250 (2016).

[28] T. A. Nieminen, N. R. Heckenberg, and H. Rubinsztein-Dunlop, J. Mod. Opt. **48**, 405 (2001).

[29] A. La Porta and M. D. Wang, Phys. Rev. Lett. **92**, 190801 (2004).

[30] Y. Arita, M. Mazilu, and K. Dholakia, Nat. Commun. **4**, 2374 (2013).

[31] T. Li, S. Kheifets, D. Medellin, and M. G. Raizen, Science **328**, 1673 (2010).

[32] T. Li, Fundamental Tests of Physics with Optically Trapped Microspheres (Springer, New York, 2013).

[33] J. Gieseler, B. Deutsch, R. Quidant, and L. Novotny, Phys. Rev. Lett. **109**, 103603 (2012).

[34] M. Li, G. W. Mulholland, and M. R. Zachariah, Aerosol Sci. Technol. **46**, 1035 (2012).

[35] J. Trojek, L. Chvátal, and P. Zemánek, J. Opt. Soc. Am. A **29**, 1224 (2012).

[36] J. Halbritter, Z. Naturforsch. A **29**, 1717 (1974).

[37] H. Cavendish, Philos. Trans. R. Soc. London **88**, 469 (1798).

[38] R. v. Eötvös, Math. Naturwiss. Ber. Ung. **8**, 65 (1890).

[39] R. A. Beth, Phys. Rev. **50**, 115 (1936).

[40] E. Adelberger, J. Gundlach, B. Heckel, S. Hoedl, and S. Schlamminger, Prog. Part. Nucl. Phys. **62**, 102 (2009).

[41] L. Haiberger, M. Weingran, and S. Schiller, Rev. Sci. Instrum. **78**, 025101 (2007).

[42] D. Rugar, R. Budakian, H. J. Mamin, and B. W. Chui, Nature (London) **430**, 329 (2004).

[43] I. Wilson-Rae, N. Nooshi, W. Zwerger, and T. J. Kippenberg, Phys. Rev. Lett. **99**, 093901 (2007).

[44] I. Wilson-Rae, N. Nooshi, J. Dobrindt, T. J. Kippenberg, and W. Zwerger, New J. Phys. **10**, 095007 (2008).

[45] H. Shi and M. Bhattacharya, J. Phys. B **49**, 153001 (2016).

[46] B. Friedrich and D. R. Herschbach, Nature (London) **353**, 412 (1991).

[47] H. Stapelfeldt and T. Seideman, Rev. Mod. Phys. **75**, 543 (2003).

[48] H. Jing, D. S. Goldbaum, L. Buchmann, and P. Meystre, Phys. Rev. Lett. **106**, 223601 (2011).

[49] C. Zhong and F. Robicheaux, arXiv:1605.03160.